

## Detection of crack in structure using dynamic analysis and artificial neural network

Manisha Maurya<sup>a</sup>, Jatin Sadarang<sup>a</sup> and Isham Panigrahi<sup>a\*</sup>

<sup>a</sup>School of Mechanical Engineering, KIIT deemed to be UNIVERSITY, Bhubaneswar, India

### ARTICLE INFO

#### Article history:

Received 15 September 2019

Accepted 6 November 2019

Available online

6 November 2019

#### Keywords:

Crack detection

Vibration analysis

FEA

Artificial neural network

### ABSTRACT

Cracks are one of the main causes of structural failure and they develop in the structures due to various reasons such as fatigue, temperature variation, excessive load, cyclic load, environmental effects, impact loading etc. Thus, structural health monitoring is necessary to avoid risks, damages and failures. So, in order to avoid an extensive failure or accident, the early prognosis of crack in structures is necessary. Visual inspection and some non-destructive testing (NDT) methods for detection of crack are difficult as it requires time, expenses and are quite inefficient. So the alternative methods are motivated to be developed. In this study, vibration analysis, finite element analysis (FEA) and an alternative way which is artificial neural network (ANN) is used to predict, detect and identify the damages in structures. It is found that the theoretical, experimental, finite element analysis and artificial neural network have good accuracy in predicting the crack characteristics.

© 2020 Growing Science Ltd. All rights reserved.

## 1. Introduction

Crack is a discontinuity in a body and is one of the main causes of structural failure and there are many research studies for crack and defect detection or characterizing the mechanical property and cracking behavior, remaining life, final load bearing capacity of cracked components and engineering materials (Scholey et al., 2009; Taheri-Behrooz et al., 2018; Wang et al., 2016,2017; Rossi & Le Maou, 1989; Aliha & Gharehbogh, 2017; Scholey et al., 2009; Abd-Elhady, 2013; Mahdavi et al., 2015; Fayed, 2018; Akbaroost, 2014; Akbaroost et al., 2014; Mirsayar et al., 2017, 2018; Mirsayar & Zollinger, 2017; Carpinteri & Ingraffea, 2012; Frommherz et al., 2016; Aliha et al., 2012, 2017a,b, 2016; Ayatollahi & Aliha 2011; Abd-Elhady, 2013; Mahdavi et al., 2015). Cracks are developed in the structures and machines due to various reasons such as fatigue, temperature variation, excessive load, cyclic load, environmental effects, impact loading, shear failure, resonance, wear corrosion, residual stress and etc. The presence of crack not only affects the stiffness of the structure but also affect the mechanical response of the whole structure to a larger extent (Prabhakar, 2009). Due to these changes, there is a reduction in modal frequencies and mode shapes. Therefore, it is feasible to anticipate the crack characteristics by determining changes in the vibration parameters (Vakil-Baghmisheh et al., 2008). Its development in a beam leads to sudden failure of a system and machines without any prior indication or warning (Satpute et al., 2017).

\* Corresponding author.  
E-mail addresses: [ipanigrahi@me.kiit.ac.in](mailto:ipanigrahi@me.kiit.ac.in) (I. Panigrahi)

Visual inspection of cracks and damages is unsuitable and not worth considering in most of the cases, thus non-destructive testing (NDT) methods like thermography, ultrasonic testing, X-ray diffraction etc. are used to predict damage in the structures. But these methods require time and expenses and are quite inefficient. So the other possible methods are motivated to be developed (Sutar et al. 2015). In this analogy the use of mathematical methods, vibration-based methods, and soft-computing techniques such as artificial neural network (a subfield of artificial intelligence) is promising and favorable.

Artificial neural networks (ANN) are mathematical model of human nerve system. Its structure is exactly identical to the biological form of the cells in human brain. It consists of a number of layers like input, hidden and output layers. The various neurons are present in each layer. The neurons in input layer represent the raw data which are fed to the system. The hidden layer is connected to the input and output layer through some weights. The neurons available in output layer represents the result of the data provided which can be represented as,

$$Y = f\left(\sum_{i=1}^n a_i w_i + b\right), \quad (1)$$

where,  $b$  = bias,  $w_i$  = weight associated with the  $i^{\text{th}}$  input,  $a_i$  = input value and  $Y$  = output of the neuron. The competence of artificial neural networks was studied by Dimarogonas (1996) for prediction of damages in structural members and rotating machinery elements. Nasiri et al. (2017) presented a review paper on the utilization of Artificial Intelligence (AI) methods for mechanical fault detection and discussed the applications of Bayesian networks, GA (genetic algorithms), fuzzy logics, case-based reasoning and ANN i.e. artificial neural networks. The behavior of the undamaged and cracked beam is compared according to the FEA results and it was found that natural frequency of transverse vibrations can be used to detect a crack in cantilever beam by Satpute et al. (2017). Sutar et al. (2015) investigated transverse crack in cantilever beam by proposing a neural network based controller. Crack stiffness to beam elemental stiffness matrix was used to obtain a homogenous linear elastic beam finite element by Teidj et al. (2016) and used the measurement of the changes in the beam frequencies and observed their variations to detect the crack defect characteristics. Thatoi et al. (2014) described the Cascade Forward Back Propagation (CFBP) network to detect cracks in structural beams with the idea of changes in the natural frequencies and their measurements. Pan et al. (2010) developed a two-stage approach combining of artificial neural network (ANN) and genetic algorithm (GA) to identify crack characteristics. The use of power series technique (PST) and ANN was analyzed by Rosales et al. (2009) for crack detection in structural beam who concluded that by the use of PST algorithm, the crack can be detected with very less errors and low cost but limits its use to simple problems like economical detection while on the other hand by the use of the ANN model, cracks with large errors can be detected and can be used for complex problems like large deformations or nonlinearities. A continuous approach for prediction of damages in beams through time-modal characteristics and artificial neural networks was presented by Park et al. (2009). Firstly, an acceleration-based neural networks (ABNN) algorithm is modeled to examine the development of crack. Secondly, a modal feature-based neural networks (MBNN) algorithm is made to detect the crack characteristics. Li et al. (2005) used a collaboration of changes in natural frequencies and strain mode shapes as input parameters in neural network for prediction of crack depth and its location in structural beams. A cantilever beam having transverse crack was used by Suresh et al. (2004) and computed the modal frequencies analytically for various crack depth and locations. These frequencies were taken as inputs to train a neural network using a modular approach with two type of architecture, specifically the multi-layer perceptron (MLP) network and radial basis function (RBF) network. Sahin & Shenoi (2003) presented an algorithm for damage detection using a collaboration of changes in natural frequencies as input parameter to the network. To check the robustness of the input data, they numerically generated a simulated arbitrary noise and added to the noise free data during training of the network. Tan et al. (2017) used the technique based on vibration, where only the first vibration mode was used to predict crack characteristics in steel beams. The modal strain energy based damage index  $\beta$  was used which is competent to detect, locate and quantify the damage. The Two-

Parameter Model (TPM) was used by Ince (2004) to model fracture in cementitious material with back propagation ANN. He summarized the use of ANN in concrete fracture problems and observed that there is no use to make material parameters assumptions as ANN directly uses the experimental values for training and testing.

## 2. Theoretical analysis

The Euler's Bernoulli beam equations are used to determine the first three natural frequency of the undamaged specimen.

$$\text{For mode 1: } \omega_{nf1} = 1.875^2 \sqrt{\frac{Eh^2}{12\rho L^4}} \quad (2)$$

$$\text{For mode 2: } \omega_{nf2} = 4.694^2 \sqrt{\frac{Eh^2}{12\rho L^4}} \quad (3)$$

$$\text{For mode 3: } \omega_{nf3} = 7.855^2 \sqrt{\frac{Eh^2}{12\rho L^4}} \quad (4)$$

where Eq. (2) to Eq. (3) are the corresponding modes of natural frequency (rad/sec) for mode 1, mode 2 and mode 3, respectively. Also, E = Young's Modulus of elasticity, h = Thickness of specimen,  $\rho$  = Density of the specimen L = Length of the specimen,  
 $\omega_{nf1} = 1/2\pi f_{n1}$ .

From the Euler formula, the natural frequency is given in radian per second to obtain it in Hz, it divided by  $2\pi$ . The modulus of the steel beam specimen is  $167.439 \times 10^9$  Pa and density is  $8169.69 \text{ kg/m}^3$ . The thickness of steel beam is 5mm, total length is 330 mm and gage length is 300 mm. 30mm of the beam was fixed at one end of the specimen such that it behaves like a cantilever beam. From the Euler's equation the first modal natural frequency of beam specimen is 40.624 Hz, second modal natural frequency is 254.606 Hz and third modal natural frequency is 712.975 Hz.

## 3. Experimental analysis through tap test

In this paper, a single cracked cantilever beam specimen as shown in Fig. 1 has been taken of following dimensions and material: Total length of beam, L = 330 mm, gage length, l = 300 mm, breadth, W = 25 mm, thickness, t = 5 mm and material is the mild steel.

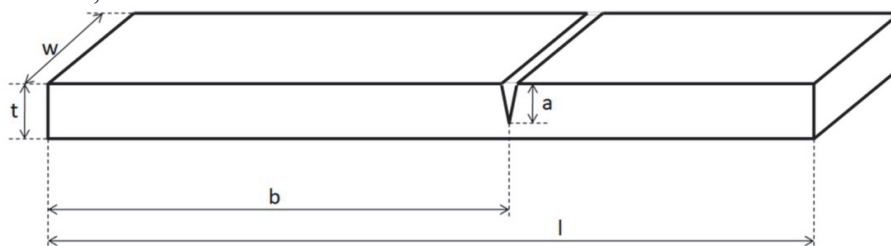


**Fig. 1.** Single cracked cantilever beam specimen.

Tap test was performed to obtain first three modal natural frequencies. Six single cracked cantilever beam specimen are taken and tap test was performed using these beams. In the experiment several crack locations from the fixed end were given in the beam. Tap test is a method used to determine the natural frequency of the beam structures. This setup as shown in Fig. 2 involved the use of a clamp (to fix the mild steel beam as a cantilever), accelerometer (PCB 353B33), connecting cables, FFT analyzer (OROS OR34- 4 channels compact analyzer) and a laptop (with FFT analyzer software NV GATE).

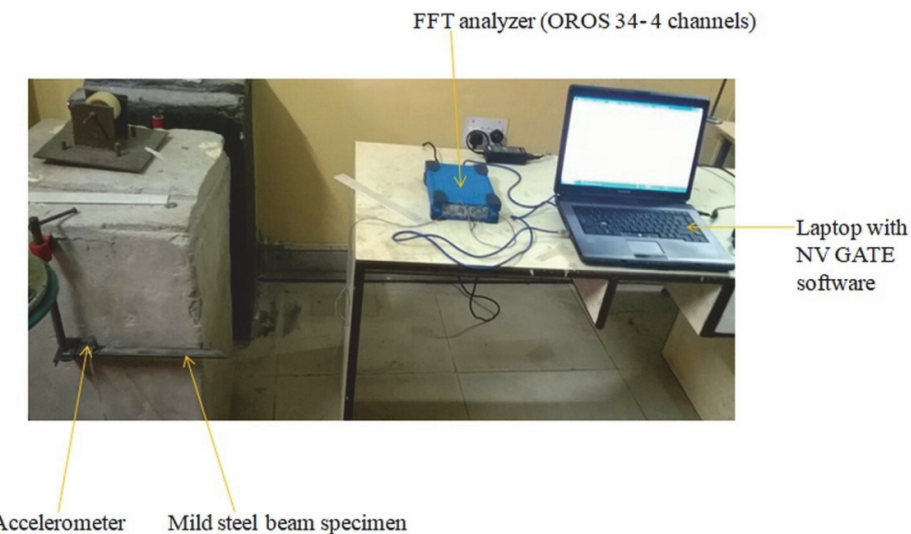


**Fig. 2.** Experimental setup.

The one end of the specimen was fixed as a cantilever beam on to the clamp, keeping a length of 300 mm of the beam to hang freely and 30 mm of the part was clamped. An accelerometer was mounted at the fixed end to obtain natural frequencies. The accelerometer data reader collects vibration acceleration data and shows it in the software. In this test, the cantilever beam was given a downward displacement of 20 mm and then released such that it vibrates freely and gets damped to its own. The corresponding vibration data was taken from the NV Gate software installed in the laptop. Readings were taken out for both damaged and undamaged beam specimens. The line diagram of the setup is also shown in Fig. 3. Here, six cracked beam as shown in Fig. 4 is taken with crack depth of 1 mm, 2 mm, 3 mm and 4 mm at various crack locations from the fixed end.

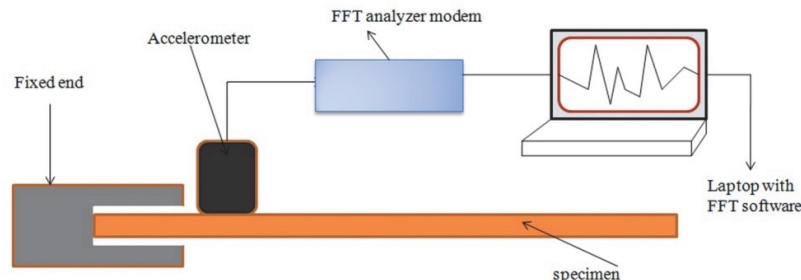


**Fig. 3.** Line diagram of setup for tap test



**Fig. 4.** Cracked beam specimens

The experimental data i.e. first three natural frequencies of undamaged and damaged beam at depth of 1mm, 2mm, 3mm and 4 mm at different locations obtained through tap test are given in Table 1. The frequencies of undamaged beam are as follows  $F_1 = 41$  Hz,  $F_2 = 256.64$  Hz and  $F_3 = 717.62$  Hz.

**Table 1.** Experimental results of cracked beam

Serial No.	$F_1$ (Hz)	$F_2$ (Hz)	$F_3$ (Hz)	$cd$ (a/t)	$cl$ (from fixed end) (b/l)
1.	40.234	249.219	695.313	1	1
2.	38.281	242.969	683.594	2	1
3.	36.718	245.703	687.69	3	1
4.	33.943	224.219	633.359	4	1
5.	35.937	238.672	693.45	3	45
6.	37.5	220.313	674.609	3	150
7.	41.012	254.297	664.063	3	225

The frequency versus acceleration graph of crack depth of 1 mm, 2 mm, 3 mm and 4 mm at fixed end and 3mm at mid, quarter and fixed quarter is shown in Fig. 5 (a,b,c,d).

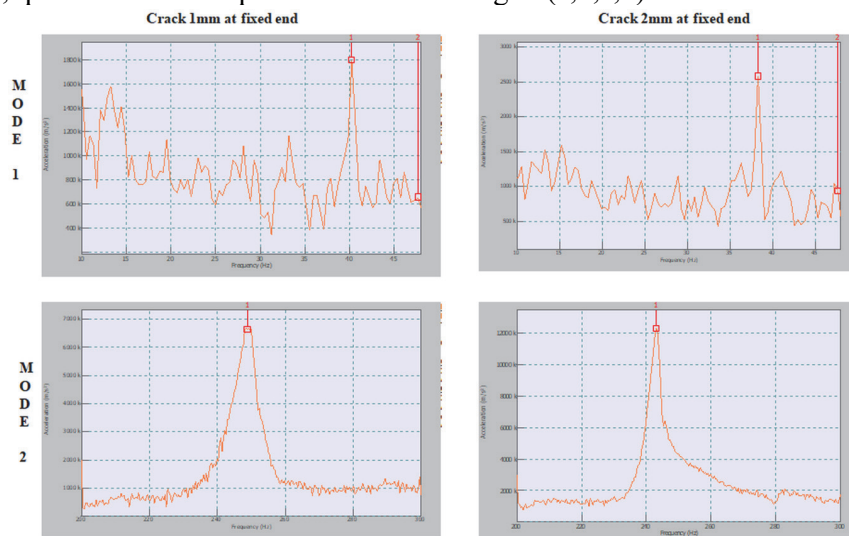


**Fig. 5(a).** Frequency Vs acceleration graph of crack depth 1mm & 2mm at fixed end

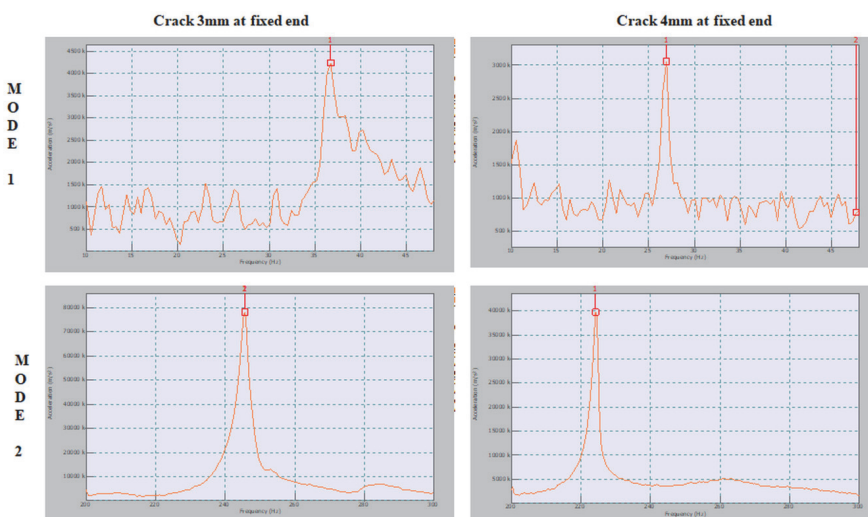


**Fig. 5(b).** Frequency Vs acceleration graph of crack depth 3mm & 4mm at fixed end

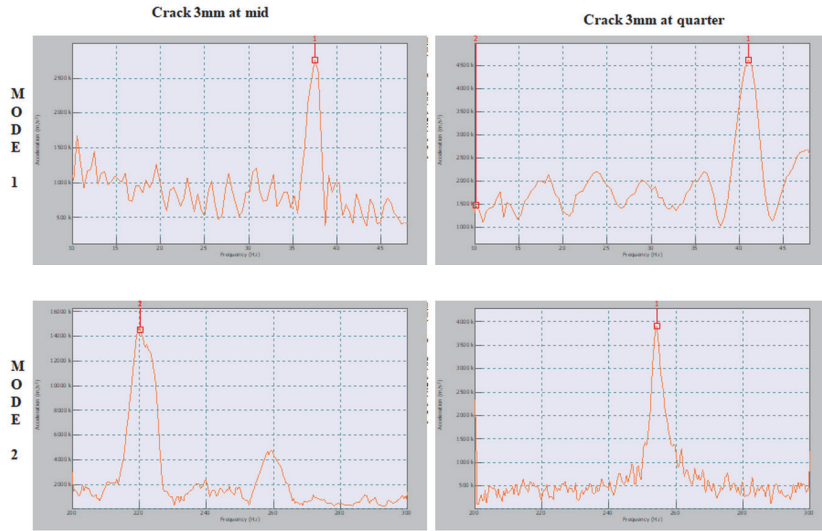


**Fig. 5(c).** Frequency Vs acceleration graph crack depth 3mm at mid & 4mm at quarter

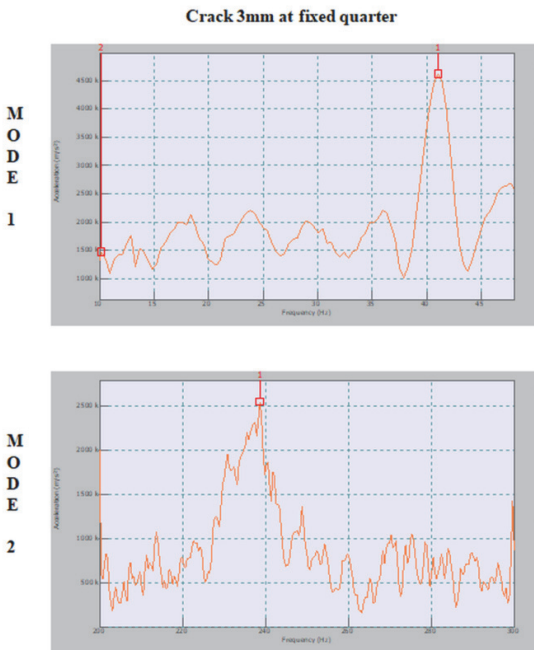


**Fig. 5(d).** Frequency Vs acceleration graph of crack depth 3mm at fixed quarter

#### 4. Finite element analysis

ANSYS is used to determine the first three modal natural frequencies of undamaged and cracked beam specimen. In model module, the material property of the specimen is given and the geometry is created of dimension of 300 mm length, 30 mm width and 5 mm thickness for undamaged specimen. The geometry of cracked specimen is same as the undamaged specimen having a crack of given depth at required locations. The thickness of crack is 0.5 mm for all cracks of depth 1mm, 2 mm, 3 mm and 4 mm. The brick elements are used to mesh the beam. Fine mesh is used in which total numbers of elements is 1800 and numbers of node is 10777. One end face of the beam specimen is fixed so that the beam behaves like a cantilever beam. Then three model natural frequencies is obtained. The first modal natural frequency of the undamaged beam specimen is 41 Hz, second model natural frequency is 255.45 Hz and third model natural frequency is 714.11 Hz.

The following Table 2 gives the FEA results i.e. first three natural frequencies and Fig. 6 shows the first three mode shapes of undamaged beam and Fig. 7(a, b, c, d) shows the mode shapes of cracked beam.

**Table 2.** FEA results of cracked beam

Serial No.	F <sub>1</sub> (Hz)	F <sub>2</sub> (Hz)	F <sub>3</sub> (Hz)	cd	cl (from fixed end)
1.	40.32	252.46	706.21	1	1
2.	39.015	245.14	687.54	2	1
3.	37.199	236.22	667.42	3	1
4.	33.01	219.87	637.72	4	1
5.	37.627	253.16	714.75	3	45
6.	40.032	235.3	715.7	3	150
7.	40.937	254.64	696.6	3	225

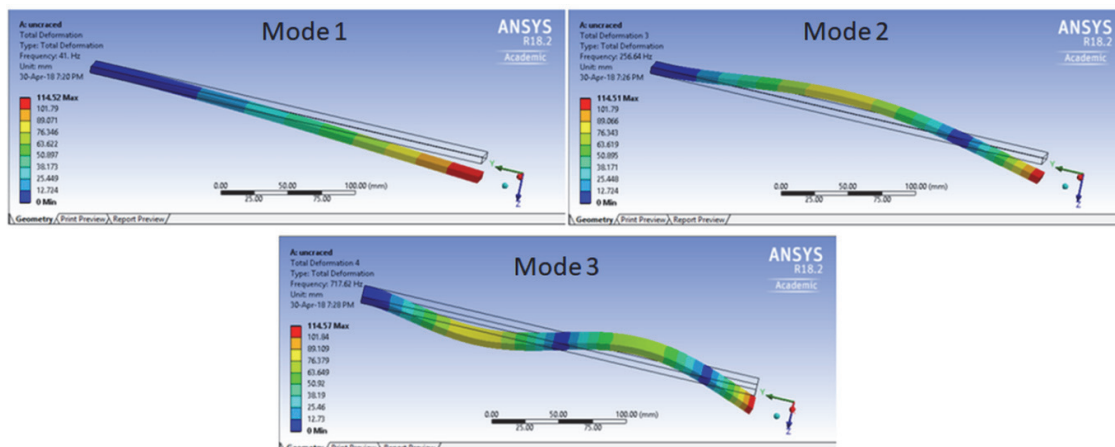


**Fig. 6.** Mode shapes of undamaged beam

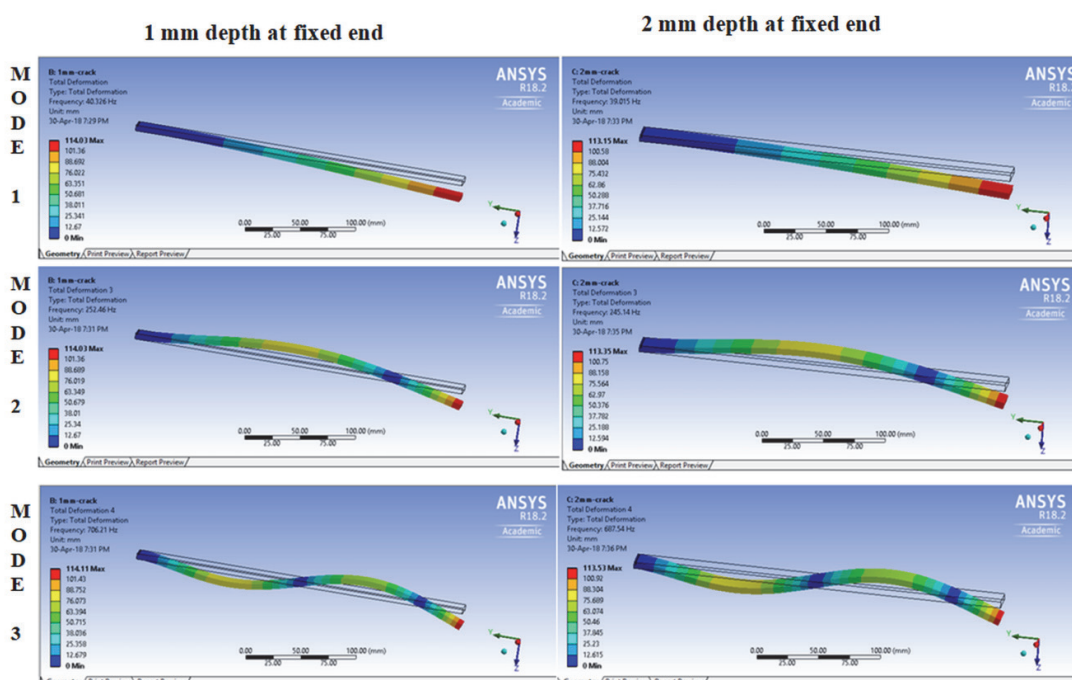


**Fig. 7(a).** Mode shapes of cracked beam

3 mm depth at fixed end

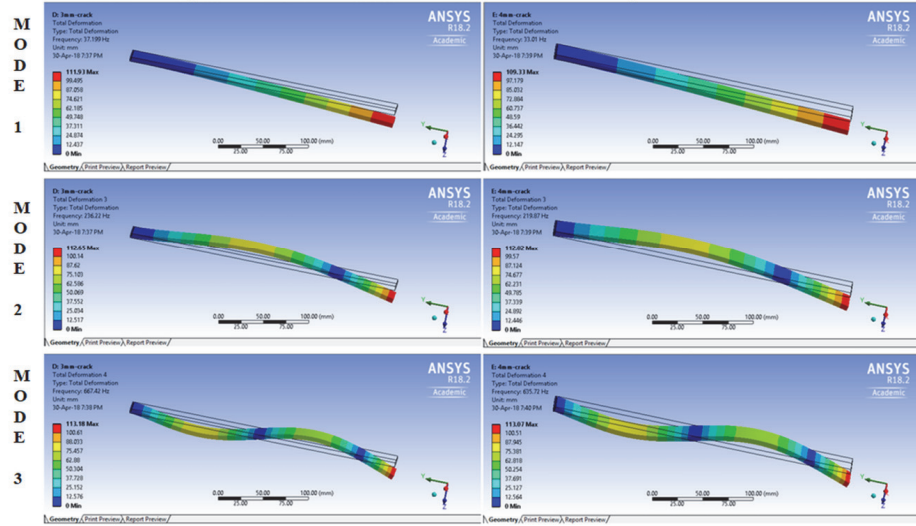


Fig. 7(b). Mode shapes of cracked beam

3 mm depth at mid from fixed end

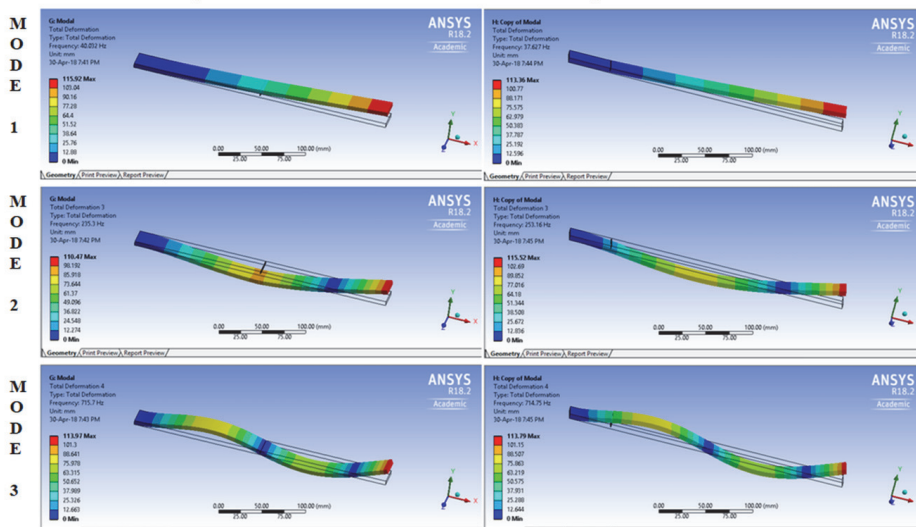


Fig. 7(c). Mode shapes of cracked beam

3 mm depth at 25 mm from fixed end

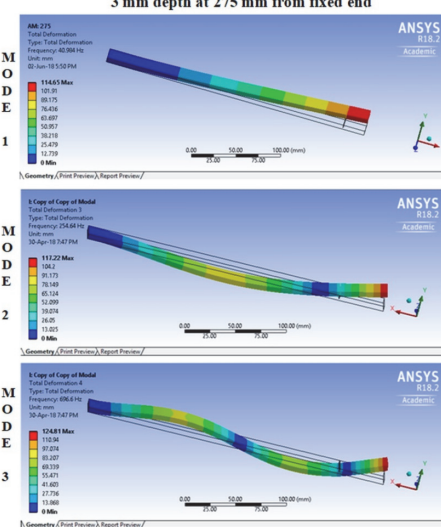


Fig. 7(d). Mode shapes of cracked beam

#### 4.1 Comparison between experimental and FEA results

The first three modal natural frequencies of beam with crack of depth of 1 mm, 2 mm, 3 mm and 4 mm at different locations are obtained from both the experimental and finite element method. The natural frequencies obtained from both the experimental and FEA methods are compared as given in Table 3.

**Table 3.** Comparison between experimental and FEA results

Serial No.	F <sub>1</sub> (EXPT.)	F <sub>1</sub> (FEA)	Error % w.r.t Expt.	F <sub>2</sub> (EXPT)	F <sub>2</sub> (FEA)	Error % w.r.t Expt.	F <sub>3</sub> (EXPT)	F <sub>3</sub> (FEA)	Error % w.r.t Expt.
1.	40.234	40.32	<b>0.213</b>	249.219	252.46	<b>1.3</b>	695.313	706.21	<b>1.567</b>
2.	38.281	39.015	<b>1.917</b>	242.969	245.14	<b>0.893</b>	683.594	687.54	<b>0.577</b>
3.	36.718	37.199	<b>1.309</b>	245.703	236.22	<b>3.859</b>	687.69	667.42	<b>2.947</b>
4.	33.943	33.01	<b>2.748</b>	224.219	219.87	<b>1.939</b>	633.359	637.72	<b>0.688</b>
5.	35.937	37.627	<b>4.702</b>	238.672	253.16	<b>6.07</b>	693.45	714.75	<b>3.071</b>
6.	37.5	40.032	<b>6.752</b>	220.313	235.3	<b>6.802</b>	674.609	715.7	<b>6.091</b>
7.	41.012	40.937	<b>0.182</b>	254.297	254.64	<b>0.134</b>	664.063	696.6	<b>4.899</b>

From the above Table 3, it is found that the maximum error percentage between the experimental and finite element analysis results is less than 7% and average error percentage for first, second and third natural frequencies are 2.54, 2.99 and 2.83 respectively. Thus, it can be seen that the experimental data are very close to the finite element analysis values hence for further prediction of crack in neural network; we can obtain the analytical values of natural frequencies at various depth and location and use it for training in neural network. This involves simplicity and less time for evaluation of natural frequencies as compared to experimental method.

#### 4.2 Other FEA data

In ANSYS, natural frequencies of beam with crack depth of 1mm, 2mm, 3mm and 4mm at every 25mm from fixed location for each depth has been obtained using modal analysis. The input and output variables have to be normalized such that it should lie in the same range group of 0 to 1. Therefore the relative values are obtained according to the equations given below:

- Relative frequency ( $f_1, f_2, f_3$ ) = frequency of cracked beam / frequency of undamaged beam
- Relative crack depth,  $cd = a / t$  = depth of crack / thickness of the beam
- Relative crack location,  $cl = b / l$  = location of crack from fixed end / length of the beam

The Table 4 gives the relative natural frequencies at desired relative depth and location. These data are used in neural networking for prediction of crack.

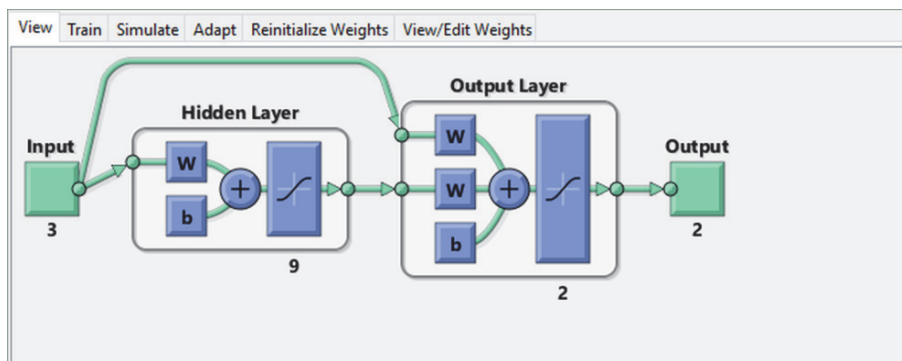
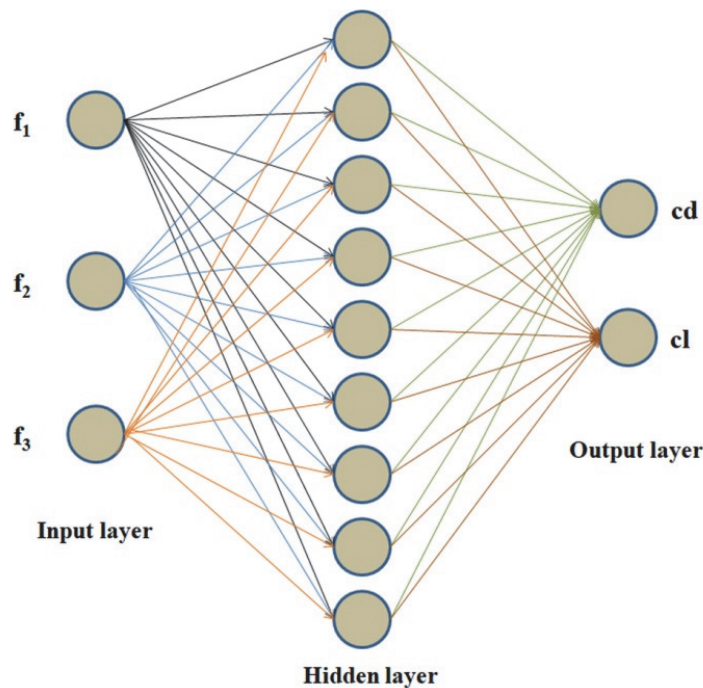
### 5. Neural network modeling

Artificial neural networking (ANN) in MATLAB is used to analyze and predict the depth and position of crack in the beam and data obtained by training is validated by the analytical results. The data given in Table 3.9 are used for training in neural network except data number 3, 8, 13, 19, 25, 31, 37, 43, 49 and 52 which are used for testing the network as 80% of the data are for training ad 20% are for testing the networks. In MATLAB, the desired inputs and outputs or targets are imported in the workspace and using “nntool” network is created using inputs and targets. Here, a typical three-layered Cascade-Forward Back Propagation (CFBP) neural network is considered consisting of three neurons in input layer, nine neurons in hidden layer and two neurons in output layer as shown in Fig. 8 and architecture is shown in Fig. 9.

**Table 4.** Relative natural frequencies at given depth and location

Serial No.	f <sub>1</sub>	f <sub>2</sub>	f <sub>3</sub>	cd	cl
1.	0.983561	0.9837126	0.9841002	0.2	0.0033
2.	0.9877561	0.9936097	0.9969482	0.2	0.0833
3.	0.9896342	0.9970776	0.9966695	0.2	0.1666
4.	0.9919268	0.99774	0.9929628	0.2	0.25
5.	0.9939024	0.9955969	0.9917784	0.2	0.3333
6.	0.9956342	0.9934149	0.9952761	0.2	0.4166
7.	0.9963171	0.9902977	0.9969761	0.2	0.5
8.	0.9971951	0.9913887	0.9943842	0.2	0.5833
9.	0.9978537	0.9929084	0.9904546	0.2	0.6666
10.	0.9980976	0.9950514	0.9898136	0.2	0.75
11.	0.9982195	0.9967269	0.9933112	0.2	0.8333
12.	0.9983659	0.9973893	0.9960564	0.2	0.9166
13.	0.9986342	0.9983635	0.9974499	0.2	0.9966
14.	0.9515854	0.9551901	0.9580837	0.4	0.0033
15.	0.9502927	0.9757637	0.988852	0.4	0.0833
16.	0.9685366	0.9952073	0.9956244	0.4	0.1666
17.	0.9748049	0.9974283	0.9810763	0.4	0.25
18.	0.9829268	0.9896743	0.9786935	0.4	0.3333
19.	0.9868049	0.9774392	0.9888938	0.4	0.4166
20.	0.9911463	0.9692176	0.9977704	0.4	0.5
21.	0.9945122	0.969841	0.9860372	0.4	0.5833
22.	0.9971463	0.9820371	0.9747499	0.4	0.6666
23.	0.9982927	0.9883494	0.9703604	0.4	0.75
24.	0.9988537	0.9961425	0.988643	0.4	0.8333
25.	0.9990732	0.9982466	0.9964048	0.4	0.9166
26.	0.9985854	0.9981686	0.9958892	0.4	0.9966
27.	0.9072927	0.9204333	0.9300465	0.6	0.0033
28.	0.884	0.9495402	0.9803099	0.6	0.0833
29.	0.8984634	0.9897132	0.9909283	0.6	0.1666
30.	0.9386829	0.9959476	0.955868	0.6	0.25
31.	0.9462683	0.96988	0.9384911	0.6	0.3333
32.	0.965561	0.9421758	0.975363	0.6	0.4166
33.	0.9756829	0.9134975	0.9976868	0.6	0.5
34.	0.9874878	0.9215243	0.9677267	0.6	0.5833
35.	0.9929024	0.9315383	0.9162927	0.6	0.6666
36.	0.9972683	0.9679707	0.9190937	0.6	0.75
37.	0.9990732	0.9907263	0.9582091	0.6	0.8333
38.	0.9996098	0.9982855	0.9941195	0.6	0.9166
39.	1.0002439	1.0009352	0.9994983	0.6	0.9966
40.	0.805122	0.8567254	0.8858727	0.8	0.0033
41.	0.669561	0.8892612	0.9618182	0.8	0.0833
42.	0.7276098	0.979855	0.9801984	0.8	0.1666
43.	0.8285854	0.9922459	0.8904016	0.8	0.25
44.	0.8213659	0.9134585	0.8500181	0.8	0.3333
45.	0.8743415	0.826956	0.934882	0.8	0.4166
46.	0.9208537	0.7783276	0.9976868	0.8	0.5
47.	0.9527317	0.78012	0.9201249	0.8	0.5833
48.	0.9804146	0.8184227	0.827764	0.8	0.6666
49.	0.9927805	0.8896898	0.7862518	0.8	0.75
50.	0.9988781	0.9760365	0.8948887	0.8	0.8333
51.	1.0000244	0.9954021	0.9743458	0.8	0.9166
52.	1.0009024	1.0015976	1.0001533	0.8	0.9966

The first three relative natural frequencies (f<sub>1</sub>, f<sub>2</sub>, and f<sub>3</sub>) are taken as input parameter; relative length (l) and relative depth (d) are taken as output parameters. The various functions used are: Levenberg Marquardt (trainlm) is taken as Training function, LEARNGDM is taken as adaption learning function, Mean square error (MSE) taken as performance function and Sigmoid function (tansig) as transfer function. The input parameters required for the training of data are provided as shown in Table 5.

**Fig. 8.** CFBP neural network**Fig. 9.** Architecture of CFBP neural network.**Table 5.** Input parameters for training

Serial No.	Input Parameters for Training	Values
1.	Goal	1e-06
2.	Learning rate	0.1
3.	Momentum parameter	0.9
4.	Number of epochs	1000
5.	Number of nodes in input layer	3
6.	Number of neuron in hidden layer	9
7.	Number of nodes in output layer	2

## 6. Validation of ANN results with FEA results

The data from the Table 4 are trained in the neural network and the outputs are predicted.

The outputs of both the analytical and predicted testing data as given above (through ANN) are compared as shown in Table 6.

**Table 6.** Comparison between FEA and ANN outputs

Data No.	cd (FEA)	cd (ANN)	Error % w.r.t FEA	cl (FEA)	cl (ANN)	Error % w.r.t FEA
3.	0.2	0.2047	<b>2.375</b>	0.1666	0.1593	<b>4.396</b>
8.	0.2	0.2119	<b>5.99</b>	0.5833	0.6376	<b>0.9794</b>
13.	0.2	0.2039	<b>1.95</b>	0.9966	0.9763	<b>2.0414</b>
19.	0.4	0.4034	<b>0.867</b>	0.4166	0.4050	<b>2.7976</b>
25.	0.4	0.4194	<b>4.87</b>	0.9166	0.9003	<b>1.783</b>
31.	0.6	0.6054	<b>0.9083</b>	0.3333	0.3337	<b>0.11</b>
37.	0.6	0.6167	<b>2.7983</b>	0.8333	0.7852	<b>5.7711</b>
43.	0.8	0.8146	<b>1.825</b>	0.25	0.2470	<b>1.172</b>
49.	0.8	0.8007	<b>0.0912</b>	0.75	0.7511	<b>0.152</b>
52.	0.8	0.8405	<b>5.0737</b>	0.9966	0.9942	<b>0.2474</b>

## 7. Results and discussion

In order to avoid an extensive failure or accident, the early prognosis of crack in structures is necessary. With the use of Euler's equation, the natural frequency of the undamaged beam is obtained and it is found that it is close to the experimental and numerical results. The experimental natural frequencies and mode shapes of six cracked beam specimens at seven different crack locations of crack depth 1mm, 2mm, 3mm and 4mm are obtained. For the same depth and location, finite element analysis results are obtained and are compared with experimental values as shown in Table 3. It is found that the error percentage between them is less than 7% which indicates that the FEA results are closer to the experimental results. Therefore, to reduce time, money and material, the finite element method is used to determine the first three modal frequencies of cracked beam for different depth and locations which are further used as inputs to the neural network for prognosis of crack.

The frequencies of cracked beam obtained from finite element analysis are trained in the Cascade Forward Back Propagation (CFBP) Neural Network. Table 6 shows us the comparison between numerical and ANN outputs. The results obtained are as follows:

- It is been seen from Table 6 that the maximum error percentage between the actual (FEA) and the predicted (ANN) outputs is less than 6 % which shows that ANN is well built to estimate the crack characteristics of cantilever cracked beam.
- The average error percentage between the FEA and ANN outputs is 2.67 for depth and 2.49 for location.

The regression analysis of training, validation and test data is shown in Fig. 10 which shows that predicted data are well fitted to the actual outputs.

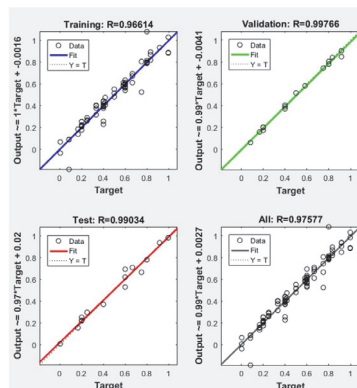


**Fig. 10.** Regression analysis

A comparison graph between FEA and ANN outputs for crack depth and crack location has been shown in Fig. 11(a) & 11(b) respectively.

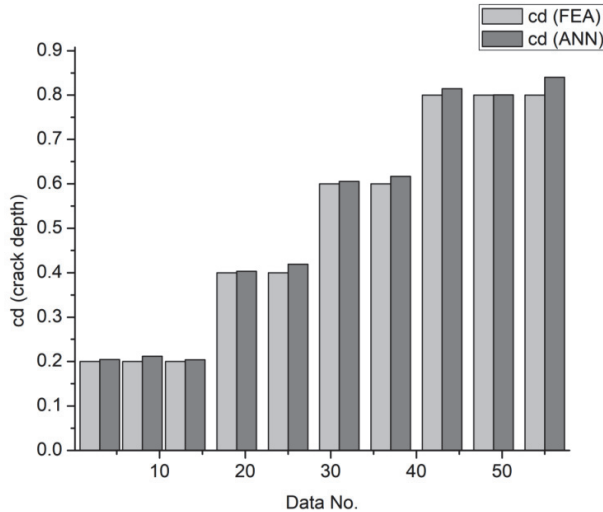


**Fig. 11(a).** Comparison graph for crack depth.

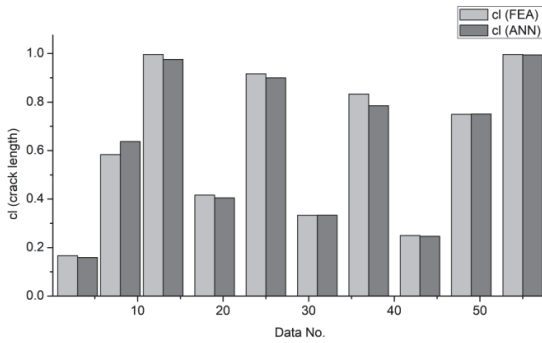


**Fig. 11(b).** Comparison graph for location.

## 8. Conclusions

Crack development in a beam leads to sudden failure of a system without any prior indication or warning. Thus, structural health monitoring is necessary to avoid risks, damages and breakdown. So, in order to avoid an extensive failure or accident, the early prognosis of crack in structures is necessary. Therefore, in this study various techniques like vibration analysis, finite element analysis (FEA) and soft computing method i.e. artificial neural network (ANN) have been used for diagnosis and identification of crack in structures. Based on this study, the following points are concluded as:

- Due to the presence of crack in structure, the natural frequency decreases and hence the stiffness of the structure also decreases.
- The maximum error percentage between the experimental and FEA results are less than 7% which indicates that both the results are in good agreement to each other. So the natural frequencies obtained by FEA can be used for training in neural network for prediction of crack which involves simplicity and less time for evaluation of natural frequencies as compared to experimental method.
- Thus, the maximum error % between the actual (FEA) and the predicted (ANN) outputs is less than 6 % which shows that ANN is well built to estimate the crack depth and location of cantilever cracked beam.
- ANN can be used to predict damages in metallic and composite structures and classify faults in rolling bearing elements with good accuracy.

- A neural controller can be programmed, trained and installed in a structure and this ANN controller will provide us the damage information accurately.

## 9. Future scope

A neural controller can be made and installed in structures using the ANN algorithm and can be programmed according to it, which can predict the damages and can provide prior warning and indication.

## References

- Abd-Elhady, A. (2013). Mixed mode I/II stress intensity factors through the thickness of disc type specimens. *Engineering Solid Mechanics*, 1(4), 119-128.
- Akbaroost, J. (2014). Size and crack length effects on fracture toughness of polycrystalline graphite. *Engineering Solid Mechanics*, 2(3), 183-192.
- Akbaroost, J., Ayatollahi, M. R., Aliha, M. R. M., Pavier, M. J., & Smith, D. J. (2014). Size-dependent fracture behavior of Guiting limestone under mixed mode loading. *International Journal of Rock Mechanics and Mining Sciences*, 71, 369-380.
- Aliha, M. R. M., & Gharehbaghi, H. (2017). The effect of combined mechanical load/welding residual stress on mixed mode fracture parameters of a thin aluminum cracked cylinder. *Engineering Fracture Mechanics*, 180, 213-228.
- Aliha, M. R. M., Berto, F., Bahmani, A., Akhondi, S., & Barnoush, A. (2016). Fracture assessment of polymethyl methacrylate using sharp notched disc bend specimens under mixed mode I+ III loading. *Physical Mesomechanics*, 19(4), 355-364.
- Aliha, M. R. M., Heidari-Rarani, M., Shokrieh, M. M., & Ayatollahi, M. R. (2012). Experimental determination of tensile strength and K (IC) of polymer concretes using semi-circular bend(SCB) specimens. *Structural Engineering and Mechanics*, 43(6), 823-833.
- Aliha, M. R. M., Mahdavi, E., & Ayatollahi, M. R. (2017b). The influence of specimen type on tensile fracture toughness of rock materials. *Pure and Applied Geophysics*, 174(3), 1237-1253.
- Aliha, M. R. M., Razmi, A., & Mansourian, A. (2017a). The influence of natural and synthetic fibers on low temperature mixed mode I+ II fracture behavior of warm mix asphalt (WMA) materials. *Engineering Fracture Mechanics*, 182, 322-336.
- Ayatollahi, M. R., & Aliha, M. R. M. (2011). On the use of an anti-symmetric four-point bend specimen for mode II fracture experiments. *Fatigue & Fracture of Engineering Materials & Structures*, 34(11), 898-907.
- Carpinteri, A., & Ingraffea, A. R. (Eds.). (2012). *Fracture mechanics of concrete: Material characterization and testing: Material Characterization and Testing* (Vol. 3). Springer Science & Business Media.
- Dimarogonas, A. D. (1996). Vibration of cracked structures: a state of the art review. *Engineering fracture mechanics*, 55(5), 831-857.
- Fayed, A. (2018). Numerical evaluation of mode I/II SIF of quasi-brittle materials using cracked semi-circular bend specimen. *Engineering Solid Mechanics*, 6(2), 175-186.
- Frommherz, M., Scholz, A., Oechsner, M., Bakan, E., & Vaßen, R. (2016). Gadolinium zirconate/YSZ thermal barrier coatings: Mixed-mode interfacial fracture toughness and sintering behavior. *Surface and coatings technology*, 286, 119-128.
- Ince, R. (2004). Prediction of fracture parameters of concrete by artificial neural networks. *Engineering Fracture Mechanics*, 71(15), 2143-2159.
- Li, H., He, C., Ji, J., Wang, H., & Hao, C. (2005). Crack damage detection in beam-like structures using RBF neural networks with experimental validation. *International Journal of Innovative Computing Information and Control*, 1(4), 625-634.

- Mahdavi, E., Obara, Y., & Ayatollahi, M. (2015). Numerical investigation of stress intensity factor for semi-circular bend specimen with chevron notch. *Engineering Solid Mechanics*, 3(4), 235-244.
- Mirsayar, M. M., Razmi, A., Aliha, M. R. M., & Berto, F. (2018). EMTSN criterion for evaluating mixed mode I/II crack propagation in rock materials. *Engineering Fracture Mechanics*, 190, 186-197.
- Mirsayar, M., Shi, X., & Zollinger, D. (2017). Evaluation of interfacial bond strength between Portland cement concrete and asphalt concrete layers using bi-material SCB test specimen. *Engineering Solid Mechanics*, 5(4), 293-306.
- Nasiri, S., Khosravani, M. R., & Weinberg, K. (2017). Fracture mechanics and mechanical fault detection by artificial intelligence methods: A review. *Engineering Failure Analysis*, 81, 270-293.
- Pan, D. G., Lei, S. S., & Wu, S. C. (2010, October). Two-stage damage detection method using the artificial neural networks and genetic algorithms. In *International Conference on Information Computing and Applications* (pp. 325-332). Springer, Berlin, Heidelberg.
- Park, J. H., Kim, J. T., Hong, D. S., Ho, D. D., & Yi, J. H. (2009). Sequential damage detection approaches for beams using time-modal features and artificial neural networks. *Journal of Sound and Vibration*, 323(1-2), 451-474.
- Prabhakar, M. S. (2009). *Vibration analysis of cracked beam* (Doctoral dissertation, Master Thesis, National Institute of Technology Rourkela, Rourkela).
- Rosales, M. B., Filipich, C. P., & Buezas, F. S. (2009). Crack detection in beam-like structures. *Engineering Structures*, 31(10), 2257-2264.
- Rossi, P., & Le Maou, F. (1989). New method for detecting cracks in concrete using fibre optics. *Materials and structures*, 22(6), 437-442.
- Sahin, M., & Shenoi, R. A. (2003). Quantification and localisation of damage in beam-like structures by using artificial neural networks with experimental validation. *Engineering Structures*, 25(14), 1785-1802.
- Satpute, D., Baviskar, P., Gandhi, P., Chavanke, M., & Aher, T. (2017). Crack detection in cantilever shaft beam using natural frequency. *Materials Today: Proceedings*, 4(2), 1366-1374.
- Scholey, J. J., Wilcox, P. D., Wisnom, M. R., Friswell, M. I., Pavier, M., & Aliha, M. R. (2009). A GENERIC TECHNIQUE FOR ACOUSTIC EMISSION SOURCE LOCATION. *Journal of Acoustic Emission*, 27.
- Suresh, S., Omkar, S. N., Ganguli, R., & Mani, V. (2004). Identification of crack location and depth in a cantilever beam using a modular neural network approach. *Smart Materials and Structures*, 13(4), 907.
- Sutar, M. K., Pattnaik, S., & Rana, J. (2015). Neural Based Controller for Smart Detection of Crack in Cracked Cantilever Beam. *Materials Today: Proceedings*, 2(4-5), 2648-2653.
- Taheri-Behrooz, F., Aliha, M. R., Maroofi, M., & Hadizadeh, V. (2018). Residual stresses measurement in the butt joint welded metals using FSW and TIG methods. *Steel and Composite Structures*, 28(6), 759-766.
- Tan, Z. X., Thambiratnam, D. P., Chan, T. H. T., & Razak, H. A. (2017). Detecting damage in steel beams using modal strain energy based damage index and Artificial Neural Network. *Engineering Failure Analysis*, 79, 253-262.
- Teidj, S., Khamlachi, A., & Driouach, A. (2016). Identification of beam cracks by solution of an inverse problem. *Procedia Technology*, 22, 86-93.
- Thatoi, D. N., Choudhury, S., Das, H. C., Jena, P. K., & Agrawal, G. (2014). CFBP Network-A Technique for Crack Detection. *Procedia materials science*, 6, 10-17.
- Vakil-Baghmisheh, M. T., Peimani, M., Sadeghi, M. H., & Ettefagh, M. M. (2008). Crack detection in beam-like structures using genetic algorithms. *Applied soft computing*, 8(2), 1150-1160.
- Wang, D., Zhang, H., Gong, B., & Deng, C. (2016). Residual stress effects on fatigue behaviour of welded T-joint: a finite fracture mechanics approach. *Materials & Design*, 91, 211-217.
- Wang, Q., Liu, X., Wang, W., Yang, C., Xiong, X., & Fang, H. (2017). Mixed mode fatigue crack growth behavior of Ni-Cr-Mo-V high strength steel weldments. *International Journal of Fatigue*, 102, 79-91.



© 2020 by the authors; licensee Growing Science, Canada. This is an open access article distributed under the terms and conditions of the Creative Commons Attribution (CC-BY) license (<http://creativecommons.org/licenses/by/4.0/>).